THE JOURNAL OF BIOLOGICAL CHEMISTRY VOL. 282, NO. 2, pp. 1352–1358, January 12, 2007


# Metacaspase Activity of *Arabidopsis thaliana* Is Regulated by *S*-Nitrosylation of a Critical Cysteine Residue*[S]

Received for publication, September 19, 2006, and in revised form, November 15, 2006 Published, JBC Papers in Press, November 16, 2006, DOI 10.1074/jbc.M608931200

**Beatrice Belenghi**[‡1,2], **Maria C. Romero-Puertas**[§1,3], **Dominique Vercammen**[‡4], **Anouk Brackenier**[‡5], **Dirk Inzé**[‡], **Massimo Delledonne**[§6], **and Frank Van Breusegem**[‡7]

*From the* [‡]*Department of Plant Systems Biology, Flanders Interuniversity Institute for Biotechnology, Ghent University, Technologiepark 927, B-9052 Ghent, Belgium and the* [§]*Dipartimento Scientifico e Tecnologico, Università degli Studi di Verona, Strada le Grazie, 15, I-37134 Verona, Italy*

**Nitric oxide (NO) regulates a number of signaling functions in both animals and plants under several physiological and pathophysiological conditions. *S*-Nitrosylation linking a nitrosothiol on cysteine residues mediates NO signaling functions of a broad spectrum of mammalian proteins, including caspases, the main effectors of apoptosis. Metacaspases are suggested to be the ancestors of metazoan caspases, and plant metacaspases have previously been shown to be genuine cysteine proteases that autoprocess in a manner similar to that of caspases. We show that *S*-nitrosylation plays a central role in the regulation of the proteolytic activity of *Arabidopsis thaliana* metacaspase 9 (AtMC9) and hypothesize that this *S*-nitrosylation affects the cellular processes in which metacaspases are involved. We found that AtMC9 zymogens are *S*-nitrosylated at their active site cysteines *in vivo* and that this posttranslational modification suppresses both AtMC9 autoprocessing and proteolytic activity. However, the mature processed form is not prone to NO inhibition due to the presence of a second *S*-nitrosylation-insensitive cysteine that can replace the *S*-nitrosylated cysteine residue within the catalytic center of the processed AtMC9. This cysteine is absent in caspases and paracaspases but is conserved in all reported metacaspases.**

Nitric oxide (NO)[8] is implicated in a number of diverse physiological and pathophysiological processes and, together with its exchangeable redox-activated forms, is now recognized as an intracellular and intercellular signaling molecule in both animals and plants (1). NO can react with a variety of molecules, including heme-containing proteins, protein- and nonprotein-associated thiol groups, and other free radicals (2). *S*-Nitrosylation, the covalent attachment of a nitrogen monoxide group to the thiol side chain of cysteine, is considered the most widespread and functionally important form of physiological NO-dependent posttranslational modification (3). *S*-Nitrosylated proteins in plants have been identified and experimental evidence of regulation through *S*-nitrosylation is currently available for only three proteins: glyceraldehyde 3-phosphate dehydrogenase (4), methionine adenosyltransferase (5), and nonsymbiotic hemoglobin (6).

Many more examples of protein *S*-nitrosylation and consequent modifications in activity have been reported in animal systems (7). Regulation of procaspase 3 is just one example of how *S*-nitrosylation can control fundamental processes, such as apoptosis: in resting cells, caspase-3 zymogens are *S*-nitrosylated at the active site cysteine, and enzyme activity is inhibited, whereas during Fas-induced apoptosis they are denitrosylated and the function of the catalytic site is regained (8).

Plant genomes do not contain structural homologs of caspases, but encode several related proteins, named metacaspases, that are also present in protozoa and fungi. Metacaspases, together with paracaspases (found in *Dictyostelium discoideum* and metazoa), have been proposed to be the ancestors of metazoan caspases and to be involved in regulation of programmed cell death processes in these lineages (9). Despite conservation of the catalytic dyad of histidine and cysteine in metacaspases, paracaspases, and caspases, their overall sequence similarity is very low. Plant metacaspase zymogens autoprocess in a manner similar to that of caspases, but their substrate specificity differs because metacaspases have an Arg/Lys-specific proteolytic activity (10). The predicted structural similarity between caspases and metacaspases suggests that the acid-base motif that favors *S*-nitrosylation of the catalytic cysteine in caspases (11) is conserved around the same residue in metacaspase. This observation prompted us to investigate the possible role of NO as a regulator of metacaspase activity in plants through *S*-nitrosylation.

* This work was supported by the Research Fund of the Ghent University (Geconcerteerde Onderzoeksacties no. 12051403) and the Young Investigators Program of the European Molecular Biology Organization (to M. D.). The costs of publication of this article were defrayed in part by the payment of page charges. This article must therefore be hereby marked "*advertisement*" in accordance with 18 U.S.C. Section 1734 solely to indicate this fact.

[S] The on-line version of this article (available at http://www.jbc.org) contains supplemental Fig. S1.

[1] These two authors contributed equally to this work.

[2] Supported by the European Union Human Resources and Mobility for an Intra-European Fellowship (MEIF-CT-2004-514418).

[3] Present address: John Innes Centre, Norwich Research Park, Colney Lane, Norwich NR4 7UH, UK.

[4] A Postdoctoral Fellow of the Research Foundation-Flanders.

[5] Supported by the Institute for the Promotion of Innovation by Science and Technology in Flanders for a predoctoral fellowship.

[6] To whom correspondence may be addressed. E-mail: massimo.delledonne@univr.it.

[7] To whom correspondence may be addressed. Tel.: 32-9-3313800; Fax: 32-9-3313809; E-mail: frank.vanbreusegem@psb.ugent.be.

[8] The abbreviations used are: NO, nitric oxide; amc, 7-amido-4-methylcoumarin; AtMC, *Arabidopsis thaliana* metacaspase; DTT, dithiothreitol; GSNO, *S*-nitrosoglutathione; MES, 2-(*N*-morpholino)ethanesulfonic acid; SNP, sodium nitroprusside; VRPR, Val-Arg-Pro-Arg; CHAPS, 3-[(3-cholamidopropyl) dimethylammonio]-1-propanesulfonate.

Supplemental Material can be found at: http://www.jbc.org/cgi/content/full/M608931200/DC1

We demonstrate that NO regulates the proteolytic activity of the *Arabidopsis thaliana* type-II metacaspase AtMC9 and that NO blocks autoprocessing and activation of the AtMC9 zymogen through *S*-nitrosylation of the catalytic cysteine residue. In contrast, the mature processed form of AtMC9 is insensitive to NO inactivation because of a second catalytic cysteine that is not susceptible to *S*-nitrosylation and thereby acts as a salvaging catalytic residue within the catalytic center of processed AtMC9.

## EXPERIMENTAL PROCEDURES

*Recombinant Wild-type and Mutant AtMC9*—The cDNA for the open reading frame of AtMC9, At5g04200, was obtained as described previously (10). Briefly, reverse transcription-polymerase chain reaction with the forward and reverse primers (5′-ATGGATCAACAAGGGATGGTC-3′ and 5′-TCAAGGTTGAGAAAGGAACGTC-3′), provided with the adequate 5′ extensions for Gateway cloning (Invitrogen) was performed and the fragment inserted into pDEST17. The plasmid was introduced into *Escherichia coli* strain BL21(DE3)pLysE and production of the $His_6$-tagged protein was induced by incubation in 0.2 mM isopropyl β-D-thiogalactopyranoside for 24 h. The protein was purified with metal ion affinity chromatography (BD Talon™, Clontech, Mountain View, CA). Protein concentration was checked by Bradford analysis (Bio-Rad) with bovine serum albumin as a standard and purity was assessed by SDS-PAGE. Point mutagenesis of AtMC9 was done with the "megaprimer" method (12). The reverse mutagenic primers used were: AtMC9C147A (5′-GACCACCACTATGGGCAGAATCAGAG-3′) and AtMC9C29A (5′-GCTTCACGGTGCCATCAATGATGTTC-3′). Bacteria were produced and purified as described for wild-type AtMC9. For the production of antisera, three times 200 μg of purified recombinant AtMC9 were used as immunogen per rabbit (Eurogentec, Seraing, Belgium).

*Transgenic Plants*—The open reading frame-encoding AtMC9, AtMC9C147A, and AtMC9C29A were cloned into the binary vector pB7GW2 via Gateway recombination. In the resulting vectors, wild-type and mutants AtMC9 were under transcriptional control of the cauliflower mosaic virus 35S promoter and the glyfosinate ammonium resistance gene was present to allow selection in planta (13). Binary constructs were transformed into *Agrobacterium tumefaciens* strain $C58C1Rif^R$[pMP90] and transgene *A. thaliana* (L.) Heynh. ecotype Columbia-0 were transformed with floral dip (14) and subsequent selection. Homozygous lines containing a single locus and displaying diverse expression levels were selected for further analysis.

*Detection of S-Nitrosylated Proteins*—Proteins from *Arabidopsis* seedlings were extracted from leaf material with 1% Nonidet P-40, 0.5% sodium deoxycholate, 0.1% SDS in phosphate-buffered saline (pH 7.4), supplemented with 10% glycerol. Protein concentration was measured by means of an adapted Lowry method (Bio-Rad) with bovine serum albumin as standard. *S*-nitrosylated proteins were purified manually as described (6). Briefly, 2 mg of protein extracts was incubated with 20 mM methyl methanthiosulfate and 2.5% SDS at 50 °C for 30 min with frequent vortexing to block free cysteine. Excess methyl methanthiosulfate was removed by protein precipitation with 2 volumes of cold acetone, and proteins were resuspended in 0.1 ml of 25 mM Hepes, 1 mM EDTA, and 1% SDS (pH 7.7) per mg of protein. After the addition of 1 mM (*N*-(6-(biotinamido)hexyl-3′-(2′-pyridyldithio)propionamide (Pierce) and 1 mM ascorbic acid, the mixture was incubated for 1.5 h at room temperature in the dark with intermittent vortexing.

For purification of biotinylated proteins, samples were diluted with 2 volumes of neutralization buffer (25 mM Hepes, 1 mM EDTA, 100 mM NaCl, and 0.5% Triton X-100 (pH 7.7)), supplemented with 140 μl of neutravidin-agarose, and incubated overnight at 4 °C. Beads were washed three times with washing buffer (600 mM NaCl in neutralization buffer), resuspended with 150 mM β-mercaptoethanol in SDS-PAGE loading buffer, incubated 5 min at 95 °C, and centrifuged for 5 min at 20,000 × *g*. The supernatant was loaded on 12% SDS-PAGE and subjected to protein gel blot analysis with specific polyclonal anti-AtMC9 antibodies (10). As negative controls, the same samples were immunoprecipitated without (*N*-(6-(biotinamido) hexyl-3′-(2′-pyridyldithio)propionamide.

Purified recombinant AtMC9 was assayed with a similar method (15): 20 μM AtMC9 was incubated with 200 μM sodium nitroprusside (SNP) or *S*-nitrosoglutathione (GSNO) in MES buffer (pH 7.5) in the dark at room temperature for 30 min, followed or not by an additional incubation for 1 h under the same conditions with 10 mM of the reducing agent dithiothreitol (DTT). Excess of reagents (GSNO/DTT) were eliminated by protein precipitation with 2 volumes of cold acetone. The recombinant proteins were subjected to the biotin-switch method, resuspended on SDS-PAGE buffer, and loaded on 12% SDS-PAGE. *S*-Nitrosylated proteins were detected with anti-biotin antibody.

*Metacaspase Activity Assay*—Assays were performed as described previously (10). Briefly, enzymes were preactivated for 15 min in the appropriate buffer containing 1 mM DTT at room temperature. Ten pmol of enzyme was added to a final assay volume of 150 μl buffer (50 mM MES, pH 5.3, 10 mM DTT, 10% sucrose, 0.1% CHAPS, 150 mM NaCl) and 50 μM substrate Ac-Val-Arg-Pro-Arg-7-amido-4-methylcoumarin (Ac-VRPR-amc). Release of fluorescent amc was measured at $\lambda_{ex}$ of 380 nm and $\lambda_{em}$ of 460 nm with a FLUOstar OPTIMA microplate reader (BMG Labtech, Offenburg, Germany). Synthetic substrate Ac-VRPR-amc was synthesized by Peptides International (Louisville, KY).

*Modeling of AtMC9*—Procaspase 7 was used as a template for the generation of a three-dimensional homology model of AtMC9 with MODELLER 8v1 (16). The template used was Bookhaven's Protein Data Bank entry 1GQF. Protein structure alignments yielded 93% similarity between AtMC9 and human paracaspase 7. Alignments of metacaspases, paracaspases, and caspases were done with ClustalW (17) according to the conservation of the secondary structure.

## RESULTS

*Nitrosylation of Cys-147 in AtMC9 Impairs Autocleavage*—First, we investigated whether AtMC9 could be *S*-nitrosylated *in vitro*. Purified recombinant AtMC9 was incubated with the transnitrosylating agent GSNO and subjected to the biotin-switch method that selectively biotinylates *S*-nitrosylated cys-

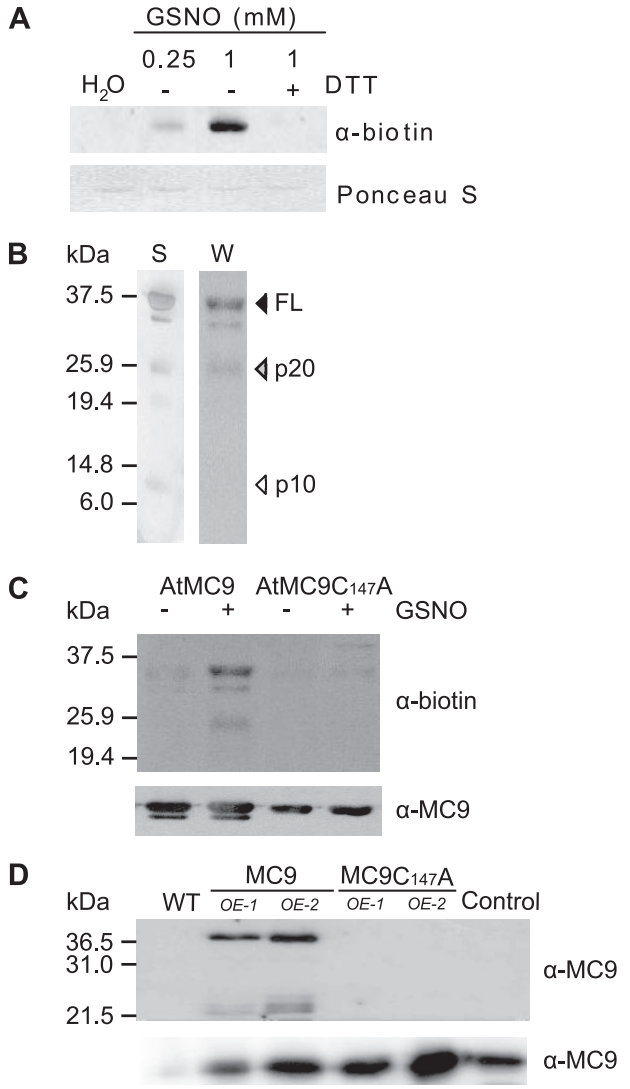


FIGURE 1. ***S*-Nitrosylation of AtMC9 *in vitro* and *in vivo*.** *A*, anti-biotin immunoblotting of purified recombinant AtMC9 (20 $\mu$M) incubated with water ($H_2O$) and GSNO (0.25 and 1 mM), followed or not by the incubation with the thiol-specific reductant DTT (10 mM), and assayed with the biotin-switch method. Ponceau S staining of polyvinylidene difluoride membranes before anti-biotin immunoblotting is shown in the *lower panel*. *B*, *S*-nitrosylation of AtMC9 full-length zymogen and p20 fragment. Purified recombinant AtMC9 (20 $\mu$M) was incubated with GSNO (200 $\mu$M), subjected to the biotin-switch assay, separated by SDS-PAGE, and stained with silver staining (*S*) or immunoblotted and visualized with anti-biotin antibody (*W*). *C*, *S*-nitrosylation of AtMC9 and AtMC9C147A mutant. Anti-biotin immunoblotting of purified recombinant AtMC9 (20 $\mu$M) and AtMC9C147A (20 $\mu$M) incubated with 200 $\mu$M GSNO (+) or water (−) and assayed by the biotin-switch method. The same membrane was reprobed with anti-AtMC9 antibody to assess protein quantity (*lower panel*). *D*, *in vivo* *S*-nitrosylation of AtMC9 and not of AtMC9C147A. Seedling extracts of two 35S::AtMC9 lines ($MC9^{OE-1}$ and $MC9^{OE-2}$), two 35S::AtMC9C147A lines ($MC9C147A^{OE-1}$ and $MC9C147A^{OE-2}$), and wild-type (*WT*) plants were subjected to the biotin-switch method. The biotinylated proteins were purified with neutravidin-agarose and immunoblotted with anti-AtMC9 antibodies. As control, nonbiotinylated proteins from a 35S::AtMC9 line were immunoprecipitated and immunoblotted (*Control*). The same protein extracts that had not been subjected to the biotin-switch were immunoblotted and probed with anti-AtMC9 antibody to assess protein expression level on the different overexpressed lines (*lower panel*).

teines (15). Protein gel blot analysis with an antibiotin antibody revealed that the full-length AtMC9 zymogen was *S*-nitrosylated and that the intensity of the signal correlated with the dosage of added GSNO (Fig. 1*A*). As expected, the signal was abolished when the thiol-specific reductant DTT was added after the GSNO treatment.

Recombinant type-II metacaspase zymogens autoprocess into a 22-kDa (p20) and a 15-kDa (p10) subunit during purification. Both subunits are expected to heterodimerize to produce the active form of the protease (10), but only the full-length protein and the p20 protein fragment were *S*-nitrosylated (Fig. 1*B* and supplemental Fig. S1*A*). The possibility that the p10 fragment was lost during the biotin-switch procedure was excluded by visualization of the fragment through silver staining. We tested the *S*-nitrosylation status of recombinant AtMC9C147A, a mutant version of AtMC9 in which the Cys residue residing in the catalytic dyad was changed into an Ala residue (10). *S*-Nitrosylation occurred predominantly at Cys-147 because the biotin-derived signal in AtMC9C147A was almost completely lost (Fig. 1*C*).

We wanted to identify AtMC9 *S*-nitrosylation *in vivo* as evidence of a possible biological function. Because endogenous AtMC9 protein levels in wild-type plants are below the detection limit by protein gel blot analysis, we used transgenic *Arabidopsis* plants carrying AtMC9 ($MC9^{OE-1}$ and $MC9^{OE-2}$) and AtMC9C147A ($MC9C147A^{OE-1}$ and $MC9C147A^{OE-2}$) under control of the constitutive cauliflower mosaic virus 35S promoter. These independent homozygous lines differ in the level of transgene expression. Until now, no aberrant phenotypes have been detected in these lines. *S*-Nitrosylated proteins in extracts from these transgenic plants were isolated by the biotin-switch method and purified with neutravidin-agarose beads. Protein gel blot analysis of purified proteins with an antibody specifically recognizing AtMC9 showed that the full-length and the p20 fragment of the AtMC9 protein were clearly visible in $MC9^{OE}$ lines, whereas in both $MC9C147A^{OE}$ lines no signal was detectable (Fig. 1*D*). These data demonstrate that also *in vivo* the zymogen of metacaspase 9 is *S*-nitrosylated at Cys-147.

We had previously shown that a mutation in the catalytic Cys-147 (AtMC9C147A) abolishes both AtMC9 autoprocessing and activity toward several synthetic fluorogenic peptide substrates (10). Subsequently, we assessed whether *S*-nitrosylation of the catalytic cysteine residues affects the autocatalytic activation of prometacaspase 9 to the mature and active form. Purified recombinant prometacaspase 9 was incubated for 15 min at pH 7.5 in the absence or presence of the NO donors SNP or GSNO before zymogen activation was triggered by switching the reaction mixture to pH 5.3 with a MES buffer. This acidic condition had been found before to be necessary for AtMC9 activation (10). Protein gel blot analysis of samples taken at 4-min intervals after the pH switch revealed a clear delay in AtMC9 autoprocessing when preincubated with SNP (Fig. 2*A*) and GSNO (data not shown). The reduced autoprocessing capacity of *S*-nitrosylated prometacaspase 9 was in accordance with a 30% reduction in activity toward an optimized synthetic tetrapeptide substrate Ac-VRPR-amc (Fig. 2*B*) (18). Oddly, an almost doubled VRPRase activity was observed when processed AtMC9 (obtained by a 15-min preincubation in the acidic assay buffer) was incubated with SNP or GSNO (Fig. 2*B*). This effect was dose-dependent up to 10 equivalent units of GSNO, while the activity decreased with higher concentrations (Fig. 2*C*),

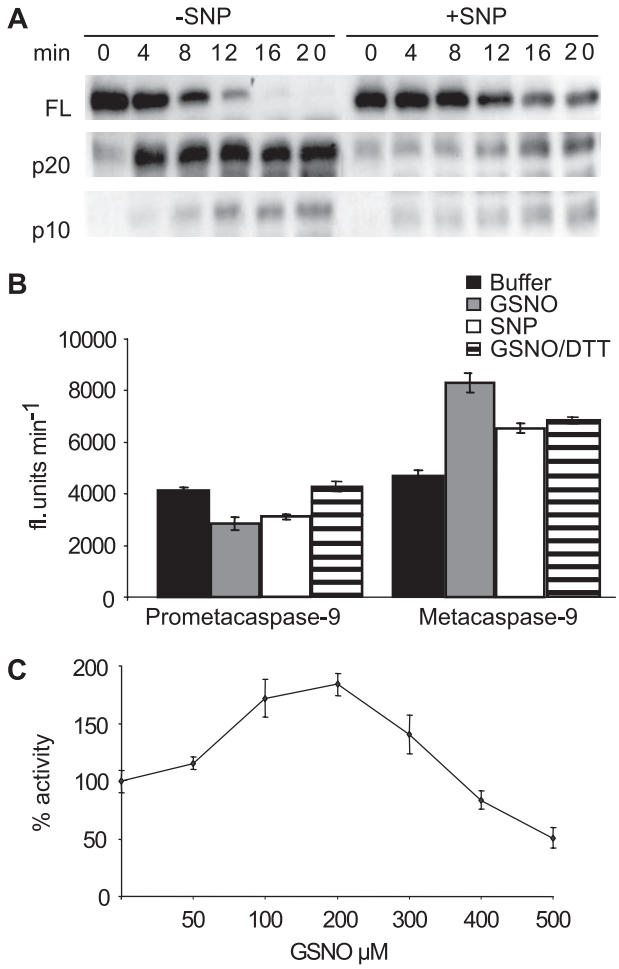


FIGURE 2. **Delay of autoprocessing of recombinant AtMC9 *in vitro* and regulation of AtMC9 activity by NO.** *A*, prometacaspase 9 (20 $\mu$M) treated without (−SNP) or with 200 $\mu$M SNP (+SNP) in Tris buffer (pH 7.5) for 15 min at room temperature before switching to MES buffer (pH 5.3). Samples were taken every 4 min after the pH switch and quenched with Laemmli buffer prior to visualization on a protein gel blot with anti-AtMC9 antibody. Bands corresponding to the full-length protein, p20, and p10 fragments are shown. *B*, activity assay with prometacaspase 9 and preactivated metacaspase 9 (20 $\mu$M) incubated in Tris buffer (pH 7.5) for 15 min without (*black columns*) or with 200 $\mu$M GSNO (*dark gray columns*) or 200 $\mu$M SNP (*white*) or with 200 $\mu$M GSNO followed by a 15-min incubation with 10 mM DTT (*striped columns*). After cold acetone precipitation and resuspension of the proteins in MES buffer (pH 5.3), the activity was measured with VRPR-amc substrate and AtMC9 assay buffer and was expressed as the increase in arbitrary fluorescent units per min. *C*, proteolytic activity of active metacaspase 9 (20 $\mu$M) incubated 15 min with different concentration of GSNO (from 0 to 300 $\mu$M). Relative activity is expressed as the percentage of the vehicle-treated control activity.

probably because of aspecific *S*-nitrosylation of all the cysteine residues present in the protein (19). Similar results were obtained with SNP (data not shown). Complete autoprocessing could be allowed (data not shown) and normal VRPRase activity (Fig. 2*B*) restored after removal of the NO group from the *S*-nitrosylated prometacaspase 9 by adding the reducing agent DTT.

*A Second Cysteine Is Involved in the Activity Mechanism of AtMC9 and Is Insensitive to S-Nitrosylation*—Strikingly, all reported protein sequences of fungal, protozoic, and plant metacaspases contain, in addition to the conserved cysteine residue in the catalytic His-Cys dyad (Cys-147 in the AtMC9 sequence), a second highly conserved cysteine residue (Cys-29 in the AtMC9) between the first strand and helix motifs (Fig. 3*A*). In caspases and paracaspases, this residue is absent. The importance of this second cysteine was first demonstrated for a *Trypanosoma brucei* metacaspase. The petite phenotype (clonal lethality and irreversibly damaged respiratory competence) obtained upon heterologous overexpression of a *T. brucei* (TbMC4) metacaspase in yeast (*Saccharomyces cerevisiae*) was not observed upon overproduction of a mutated protein in which the corresponding Cys-29 and the adjacent Cys residues were replaced by an Ala (20). To assess the functionality of this second conserved cysteine residue in plant metacaspases and its possible salvaging role in the *S*-nitrosylated form, we produced and purified three different N-terminal $His_6$-tagged mutant versions of AtMC9 in which the catalytic Cys-147 (AtMC9C147A), the second conserved cysteine (AtMC9C29A), or both cysteines (AtMC9C147AC29A) were mutated to an Ala.

During AtMC9 zymogen autoprocessing, together with p20 and p10 subunit formation, the $His_6$ tag was cleaved from the N-terminal end as evidenced by protein gel blot analysis with an anti-His antibody. This event produced five different protein fragments, corresponding to the full-length and the p20 fragment, with and without a $His_6$ tag (Fig. 3*B*), and the p10. $His_6$ cleavage occurred either at $LYKK_{-5}$, a peptide signature artificially introduced into the expression vector by Gateway cloning of the AtMC9 open reading frame, or alternatively at an internal putative cleavage site close to the N-terminal end, $VKKR_{10}$ (10). While the mutant version AtMC9C147A remained unprocessed and inactive (10), AtMC9C29A performed autoprocessing, but the resulting protein fragment signature differed from that of the wild-type AtMC9. This mutant was unable to cleave at one or both of the potential N-terminal cleavage sites ($LYKK_{-5}$ and $VKKR_{10}$) in the vicinity of the N-terminal His tag, thus producing only one p20 subunit. The full-length and p20 subunit fragments were recognized by both the anti-His and the specific anti-AtMC9 antibody (46 and 28 kDa, respectively; Fig. 3*B*), confirming that the corresponding fragments without $His_6$ tag were not produced. Processed AtMC9C29A had only 10% of VRPRase activity compared with that of the wild-type AtMC9 (Fig. 4*A*). This drastic loss of activity indicates either a fundamental role for Cys-29 in substrate cleavage or an inhibitory effect of the N-terminal peptide. To exclude this latter possibility, we tested whether AtMC9C147A, which is unable to cleave itself, and AtMC9C29A, which does not cleave the N-terminal peptide, were both able to cleave the VRPR substrate once correctly processed. Therefore, we supplemented both mutant versions with a minimal amount of readily activated recombinant wild-type AtMC9 and incubated the resulting mix for 1 h to allow complete processing. Protein gel blot analysis with an anti-AtMC9 antibody showed a correct cleavage pattern and correct maturation of all mutant proteins (Fig. S1*B*–S1*E*). VRPRase activity of both AtMC9C147A and AtMC9C29A had strongly increased, whereas in the double mutant AtMC9C147AC29A no activity was observed (Fig. 4*A*). These data confirm that at least one of the two cysteines is needed for protease activity.

We also studied the effect of *S*-nitrosylation on the activity of the different processed AtMC9 mutant forms by adding SNP

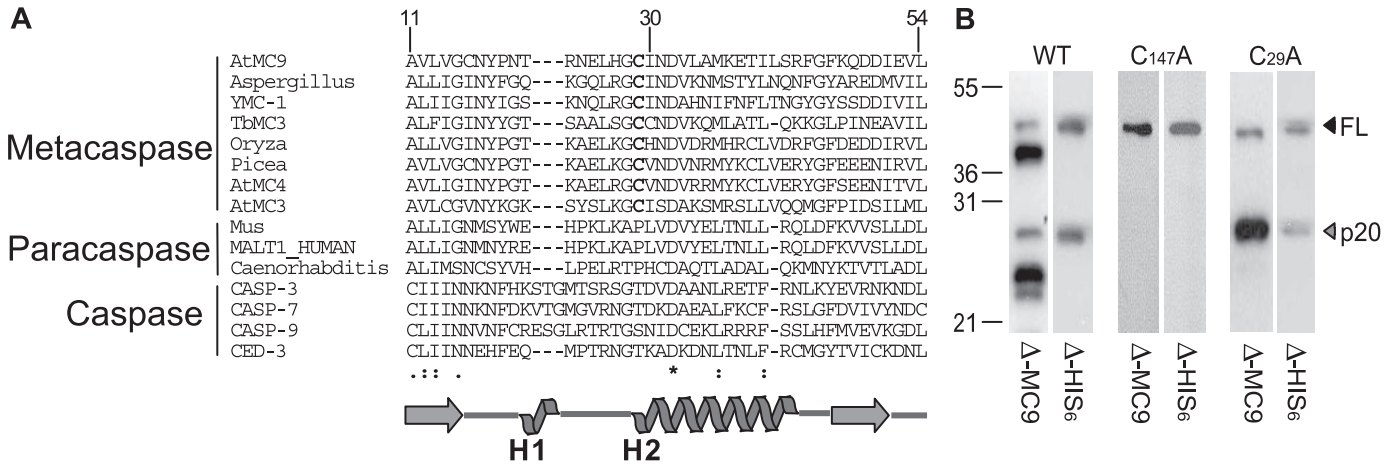


FIGURE 3. **Alignment of members of the C14 family and processing signature of wild-type and mutant forms of AtMC9.** *A*, the region surrounding the second catalytic cysteine from amino acids 11 to 54 on AtMC9 numbering is shown. The conserved cysteine is indicated in *bold*. The secondary structure of caspase 7 is given below the sequences. The symbols under the sequences denote the degree of conservation of the residues on the above column: *asterisks*, residues identical in all sequences of the alignment; *colon*, conserved substitutions observed; and *full stop*, semiconserved substitutions. *Aspergillus*, *Aspergillus nidulans* Q5B168; *YMC-1*, *S. cerevisiae* Q08601; *TbMC3*, *T. brucei* Q8T8E6; *Oryza*, *Oryza sativa* Q8LJ88; *Picea*, *P. abies* CAD59226; *AtMC4*, *A. thaliana* AAP44517; *AtMC9*, *A. thaliana* AAP44522; *AtMC3*, *A. thaliana* AAP44516; *Mus*, *Mus musculus* Q8BFT0; *MALT1_HUMAN*, *Homo sapiens* Q9UDY8; *Caenorhabditis*, *Caenorhabditis elegans* Q19719; *CASP-3*, *H. sapiens* P42574; *CASP-7*, *H. sapiens* P55210; *CASP-9*, *H. sapiens* P55211; *CED-3*, *C. elegans* P42573. *B*, processing signatures of AtMC9, AtMC9C147A, and AtMC9C29A. Recombinant AtMC9, AtMC9C147A, and AtMC9C29A were separated by SDS-PAGE and immunoblotted with polyclonal anti-AtMC9 or anti-$His_6$ antibodies. Full-length (*FL*) and p20 fragments (*p20*) are indicated.

for 20 min. Incubation of AtMC9C147A with SNP caused only a minor inhibition of the activity compared with the untreated one (Fig. 4*B*). This inhibition could be attributed to some minor and aspecific *S*-nitrosylation of the remaining cysteine residues. In contrast, *S*-nitrosylation of the AtMC9C29A mutant inhibited the activity by 75% (Fig. 4*B*). *S*-Nitrosylation of this mutant was confirmed by the biotin-switch assay (Fig. S1*D*).

## DISCUSSION

We provide both *in vitro* and *in vivo* evidence for *S*-nitrosylation of the *Arabidopsis* type-II metacaspase 9 and for a post-translational role of *S*-nitrosylation on regulation of metacaspase activity. Metacaspases are members of the CD clan of cysteine proteases encompassing also caspases, paracaspases, legumains, gingipains, separases, and clostripains (21) that have originally been proposed to be the plant functional homologs of mammalian caspases as regulators or executors of cell death (22). Functional evidence supporting this hypothesis has first been shown in the yeast YCA1 and *T. brucei* metacaspases (20, 23). In Norway spruce (*Picea abies*), metacaspases maintain the balance between differentiation and cell death during embryogenesis (24). In *Arabidopsis*, mere overproduction of AtMC9 does not lead to obvious cell death-related phenotypes, suggesting that its proteolytic activity is inhibited. Our data indicate that *in planta S*-nitrosylation of metacaspases can contribute to maintain this inhibition by impairing autocleavage and, thus, avoiding inappropriate activation. Through basal NO levels, which are provided by a constitutive production driven by NO synthase activities (25), and by enzymatic and nonenzymatic reduction of nitrite (26), Cys-147 might be *S*-nitrosylated in AtMC9 and kept in its inactive unprocessed zymogenic form. Because DTT was able to activate AtMC9 autoprocessing as well as the enzymatic activity of the *S*-nitrosylated zymogenic form, denitrosylation could push AtMC9 toward its active state. *In vivo*, denitrosylation might be accomplished by endogenous or external stimuli that can perturb the cellular redox balance. In these events, redox enzymes, such as thioredoxin or glutaredoxin, might catalyze the reaction (19). Alternatively, *S*-nitrosylated AtMC9 might be activated through cleavage by an upstream protease. In accordance with caspase cascade models, primary suspects are the type-I metacaspases that, like initiator caspases, contain an N-terminal prodomain that could be involved in regulatory protein-protein interactions (9). Functional relevance of AtMC9 (de)nitrosylation events in plants is supported by the spatio-temporal coincidence of NO accumulation and AtMC9 gene expression. AtMC9 expression is highest in xylem elements and during lateral root formation, while the AtMC9 proteolytic activity levels are above all detected during the first days of seedling germination.[9] In parallel, NO has been demonstrated before to primarily accumulate and exert a regulatory role during seed germination (27), lateral root development (28), and xylem differentiation (29). NO and *S*-nitrosylation are crucial elements in keeping human caspases permanently in an inactive form. Even after processing, caspase-3 activity is blocked when the thiol side chain of its catalytic cysteine residue is *S*-nitrosylated. The reason for this strict inhibition is the inability of the catalytic cysteine to act as a nucleophile within the proteolytic reaction scheme (15). Unexpectedly, *S*-nitrosylation does not affect AtMC9 activity in its processed mature form. We demonstrated that a second catalytic cysteine that resides in the vicinity of the genuine catalytic center can function as alternative nucleophile in AtMC9 when Cys-147 is *S*-nitrosylated. This second catalytic cysteine residue (Cys-29 in AtMC9) is highly conserved in all known metacaspases but absent in all members of the caspase and paracaspase families. This "salvage" cysteine is insensitive to *S*-nitrosylation and can rescue

[9] D. Vercammen and B. Belenghi, unpublished results.

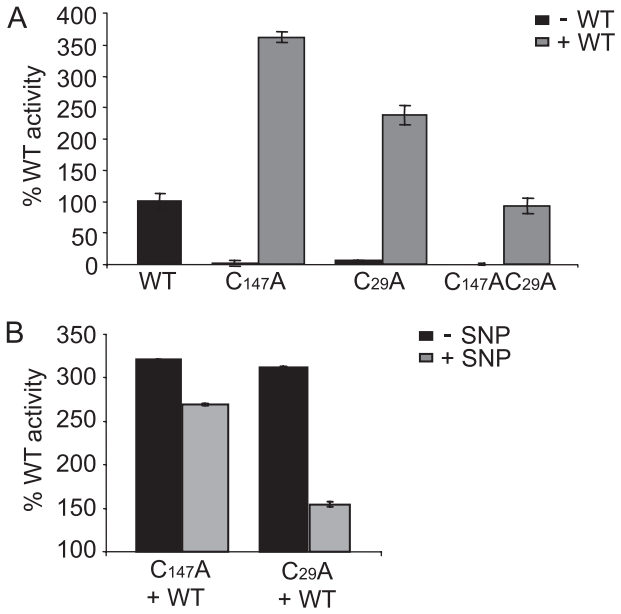


FIGURE 4. **AtMC9C147A and AtMC9C29A activation after processing by AtMC9.** *A*, proteolytic activity of AtMC9C147A, AtMC9C29A, and AtMC9C147AC29A measured 1 h after incubation with AtMC9 (ratio 4:1) in an activity assay under AtMC9 buffer conditions and VRPR-amc as substrate. Activity assay with AtMC9 (3 pmol) preactivated in assay buffer (*WT*), AtMC9C147A (12 pmol) incubated with AtMC9 (3 pmol) or without (C147A), AtMC9C29A (12 pmol) incubated with AtMC9 (3 pmol) or without (C29A), and AtMC9C147AC29A (12 pmol) incubated with AtMC9 (3 pmol) or without (C147AC29A) are shown. Relative activity is expressed as the percentage of the wild-type AtMC9 activity. *B*, proteolytic activity of AtMC9C147A and AtMC9C29A measured after 1 h of incubation with AtMC9 (ratio 4:1) as in *A* and 20-min incubation without or with 200 $\mu$M (+SNP) in an activity assay under AtMC9 buffer conditions and with VRPR-amc as substrate. Relative activity is expressed as the percentage of the wild-type AtMC9 activity for the vehicle-treated samples and of the wild-type AtMC9 + SNP activity for the SNP-treated samples.

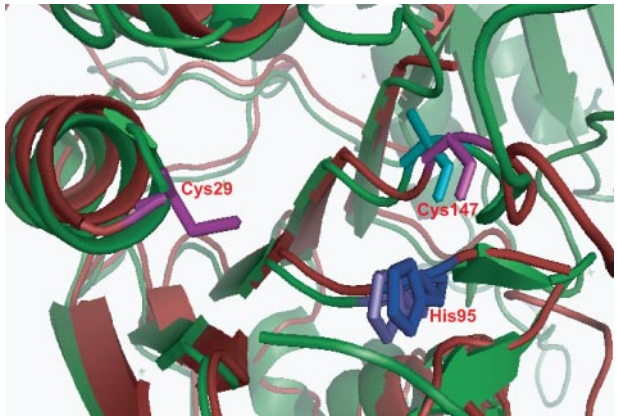


FIGURE 5. **Tertiary structure of AtMC9.** The three-dimensional structure of AtMC9 (in *red*) was predicted with human procaspase 7 (in *green*) as model. The catalytic groove is represented and the amino acids involved in the catalysis are shown in sticks: for AtMC9, Cys-29 and Cys-147 are in *violet* and His-95 in *blue*; for procaspase 7, Cys-186 is in *cyan*, and His-144 is in *purple*. The figure was drawn with the Pymol viewer (31).

the *S*-nitrosylated catalytic Cys-147 within the canonical His-Cys dyad even in the presence of high levels of NO, allowing fine-tuning of the regulation of AtMC9 activity, particularly in a cellular environment with high NO levels. In the absence of an upstream activator protease, AtMC9 is locked in its inactive proform. However, once processed by such a protease, AtMC9 is insensitive to and even more active (Fig. 2*B*) in a high NO environment.

A prediction of the three-dimensional protein structure of the AtMC9 zymogen with the known crystal structure of human procapase 7 as a template confirms the proposed tertiary structure homology of metacaspases with animal caspases (9) (Fig. 5). This structure suggests that Cys-29 is located within the catalytic groove in close proximity of the canonical catalytic residues Cys-147 and His-95, explaining the rescuing role of Cys-29. When Cys-147 is *S*-nitrosylated, AtMC9 can use the second cysteine as an alternative nucleophile for catalyzing the proteolytic reaction, while in non-*S*-nitrosylated AtMC9, it can also act as a catalytic cysteine because the AtMC9C29A mutant, once correctly processed, displays more than 50% activity (Fig. 4*A*).

Despite its predicted position within the catalytic groove and its salvage capacity in the processed AtMC9 form, Cys-29 is not able to substitute for the catalytic role of Cys-147 during autoprocessing, as illustrated by the inability of the AtMC9C147A to autoprocess and by its complete proteolytic inactivity. Only after processing, Cys-29 can substitute for Cys-147 as a catalytic residue that can be explained by the distance of Cys-29 from His-95 (7.49 Å) in the zymogen that might be too long for these two residues to interact. Once processed, conformational changes, as also described for human procaspase 7 (30), may correctly position Cys-29 within the catalytic groove. The insensitivity of Cys-29 to *S*-nitrosylation is probably due to a different charged area surrounding the Cys-29. In AtMC9, the NO-sensitive Cys-147 is surrounded by basic (His-148) and acid (Asp-145) amino acids located at 1.23 and 8.23 Å, respectively. This surrounding environment promotes a concerted acid-base catalysis of protein transnitrosylation by facilitating, on the one hand, the $H^+$ release of the SH group of Cys-147 and, on the other hand, the donation of $NO^+$ from the NO donor (3). In contrast, the surrounding area of Cys-29, with more distant acidic and basic amino acids, is unfavorable for *S*-nitrosylation. Obviously, experimental determination of the tertiary structure of AtMC9 will consolidate this hypothesis and might provide additional insights into the proteolytic mechanism of metacaspases.

In summary, we demonstrate that, like mammalian caspases, plant metacaspases can be kept inactive through *S*-nitrosylation of a critical Cys residue but are insensitive to *S*-nitrosylation when matured. We speculate that this rather surprising discrepancy is related to differences in NO householding between plants and mammals. Whereas mammals control internal NO levels very tightly by fine regulation of the activity of the various NO synthase isoforms, plants must deal with atmospheric NO as well as with internal leakage of NO that accumulates under normal growth conditions because of its production from nitrite (1). Therefore, plant metacaspases might have adapted to the NO-dependent regulatory mechanism known in human caspase 3 to function properly.

*Acknowledgments—We thank Dr. Joris Messens for helpful comments and Dr. Martine De Cock for assistance in preparing the manuscript.*

## REFERENCES


1. Delledonne, M. (2005) *Curr. Opin. Plant Biol.* **8,** 390–396
2. Stamler, J. S., Jaraki, O., Osborne, J., Simon, D. I., Keaney, J., Vita, J., Singel, D., Valeri, C. R., and Losvalzo, J. (1992) *Proc. Natl. Acad. Sci. U. S. A.* **89,** 7674–7677
3. Hess, D. T., Matsumoto, A., Kim, S. O., Marshall, H. E., and Stamler, J. S. (2005) *Nat. Rev. Mol. Cell Biol.* **6,** 150–166
4. Lindermayr, C., Saalbach, G., and Durner, J. (2005) *Plant Physiol.* **137,** 921–930
5. Lindermayr, C., Saalbach, G., Bahnweg, G., and Durner, J. (2006) *J. Biol. Chem.* **281,** 4285–4291
6. Perazzolli, M., Dominici, P., Romero-Puertas, M. C., Zago, E., Zeier, J., Sonoda, M., Lamb, C., and Delledonne, M. (2004) *Plant Cell* **16,** 2785–2794
7. Stamler, J. S., Lamas, S., and Fang, F. C. (2001) *Cell* **106,** 675–683
8. Mannick, J. B., and Schonhoff, C. M. (2004) *Free Radic. Res.* **38,** 1–7
9. Uren, A. G., O'Rourke, K., Aravind, L., Pisabarro, M. T., Seshagiri, S., Koonin, E. V., and Dixit, V. M. (2000) *Mol. Cell* **6,** 961–967
10. Vercammen, D., van de Cotte, B., De Jaeger, G., Eeckhout, D., Casteels, P., Vandepoele, K., Vandenberghe, I., Van Beeumen, J., Inzé, D., and Van Breusegem, F. (2004) *J. Biol. Chem.* **279,** 45329–45336
11. Brüne, B., and Mohr, S. (2001) *Curr. Protein Peptide Sci.* **2,** 61–72
12. Colosimo, A., Xu, Z., Novelli, G., Dallapiccola, B., and Gruenert, D. C. (1999) *BioTechniques* **26,** 870–873
13. Karimi, M., Inzé, D., and Depicker, A. (2002) *Trends Plant Sci.* **7,** 193–195
14. Clough, S. J., and Bent, A. F. (1998) *Plant J.* **16,** 735–743
15. Jaffrey, S. R., Erdjument-Bromage, H., Ferris, C. D., Tempst, P., and Snyder, S. H. (2001) *Nat. Cell Biol.* **3,** 193–197
16. Šali, A., and Blundell, T. L. (1993) *J. Mol. Biol.* **234,** 779–815
17. Chenna, R., Sugawara, H., Koike, T., Lopez, R., Gibson, T. J., Higgins, D. G., and Thompson, J. D. (2003) *Nucleic Acids Res.* **31,** 3497–3500
18. Vercammen, D., Belenghi, B., van de Cotte, B., Beunens, T., Gavigan, J.-A., De Rycke, R., Brackenier, A., Inzé, D., Harris, J. L., and Van Breusegem, F. (2006) *J. Mol. Biol.* **364,** 625–636
19. Mitchell, D. A., and Marletta, M. A. (2005) *Nat. Chem. Biol.* **1,** 154–158
20. Szallies, A., Kubata, B. K., and Duszenko, M. (2002) *FEBS Lett.* **517,** 144–150
21. Mottram, J. C., Helms, M. J., Coombs, G. H., and Sajid, M. (2003) *Trends Parasitol.* **19,** 182–187
22. Woltering, E. J., van der Bent, A., and Hoeberichts, F. A. (2002) *Plant Physiol.* **130,** 1764–1769
23. Madeo, F., Herker, E., Maldener, C., Wissing, S., Lächelt, S., Herlan, M., Fehr, M., Lauber, K., Sigrist, S. J., Wesselborg, S., and Fröhlich, K.-U. (2002) *Mol. Cell* **9,** 911–917
24. Bozhkov, P. V., Suarez, M. F., Filonova, L. H., Daniel, G., Zamyatnin, A. A., Jr., Rodriguez-Nieto, S., Zhivotovsky, B., and Smertenko, A. (2005) *Proc. Natl. Acad. Sci. U. S. A.* **102,** 14463–14468
25. Crawford, M. N. (2006) *J. Exp. Bot.* **57,** 471–478
26. Planchet, E., Gupta, K. J., Sonoda, S., and Kaiser, W. M. (2005) *Plant J.* **41,** 732–743
27. Bethke, P. C., Badger, M. R., and Jones, R. L. (2004) *Plant Cell* **16,** 332–341
28. Correa-Aragunde, N., Graziano, M., and Lamattina, L. (2004) *Planta* **218,** 900–905
29. Gabaldón, C., Gómez Ros, L. V., Pedreño, M. A., and Barceló, A. R. (2005) *New Phytol.* **165,** 121–130
30. Riedl, S. J., Fuentes-Prior, P., Renatus, M., Kairies, N., Krapp, S., Huber, R., Salvesen, G. S., and Bode, W. (2001) *Proc. Natl. Acad. Sci. U. S. A.* **98,** 14790–14795
31. DeLano, W. L. (2000) *The PyMol Molecular Graphics System*, DeLano Scientific, San Carlos, CA